BASELINE ESTIMATION IN INTERFEROMETRIC SAR

Kuldip Singh, Nicolas Stussi, Kwoh Leong Keong and Lim Hock

Center for Remote Imaging Sensing and Processing, CRISP

National University of Singapore, Lower Kent Ridge Road

119260 Singapore. Republic of Singapore

Tel: (65) 771 5070, Fax: (65) 775 77 17

E-mail: crssingh nus.sg

Abstract

In this paper we propose a new method of determining the baseline in SAR Interferometry. In particular, we show how the baseline parameters can be retrieved from a Fourier analysis of the interferometric fringes.

1. INTRODUCTION

The use of spaceborne Synthetic Aperture Radar (SAR) has been widely demonstrated as an important tool in the arena of global remote sensing. Operating in the microwave band of the electromagnetic spectrum, these radars are essentially active imaging devices, with information of the ground gathered from the echoed pulses of the radar beam. The processing of these echoes, yields not only amplitude values, which when displayed give the characteristic SAR image, but also phase information. Indeed the *complex* data which characterizes the ground reflectivity also embodies topographical information of the underlying terrain. The utility of this phase information was first demonstrated by Graham [1] where he used two vertically separated airborne antennas to receive simultaneously backscattered signals from the terrain. By coherently adding the signals recieved, he was able to produce a pattern of nulls similar to interferometric fringes observed in optical work. He further demonstrated that these fringes could be used in conjunction with the range information to yield height profiles of the terrain. This technique which forms the basis of what is called SAR Interferometry or INSAR for short, has also been employed in spaceborne systems. In such systems the separation of the antennas, called the *baseline* is obtained by utilizing a single antenna in a repeat pass [2,3].

To convert the interferomeric phases to absolute surface heights, it has been shown [4] that an accurate determination of the baseline is required. While baselines can be estimated from orbit ephemerides, the uncertainties associated with some of these parameters may introduce errors that may be unacceptable for most INSAR applications. For instance in differential inteferometry work where measurements of earth displacements of the order of a few centimeters are required [5], a high level of accuracy in the baseline is often needed.

In this contribution we examine the issue of baseline computation. In this regard we provide a theoretical framework in which the baseline can be accurately determined from a given interferogram. The method proposed here is suitable for applications such as differential interferometry where knowledge of the ground terrain (DEM) is assumed to be known.

2. SAR INTERFEROMETRY

We begin with a brief overview of SAR Interferometry that will be relevent to our analysis. Consider two radar systems S_1 and S_2 , separated by a baseline vector $\boldsymbol{b}$ illuminating the same ground area as illustrated in Fig.1.

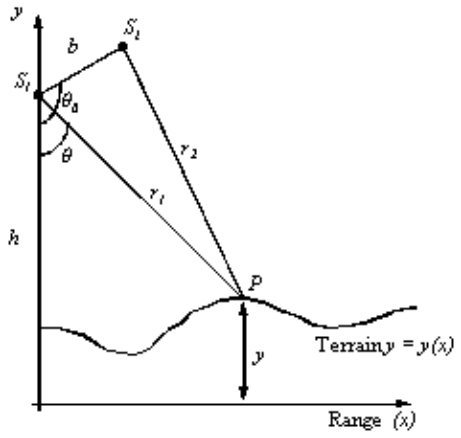

Fig.1: Typical geometry of a cross-track interferometric SAR

For a typical ground point *P* with elevation height *y* the interferometric phase $_1$ ($_2$) associated with a signal transmitted and recieved at S_1 (S_2) is

$$\phi_{1(2)} = \frac{4\pi}{\lambda} \cdot r_{1(2)} \qquad (1)$$

where $r_{1(2)} = |\boldsymbol{r}_{1(2)}|$ and is the wavelength of the radar system. Now the phase difference between the two pulses is given by

(2)

$$\phi = \phi_1 - \phi_2$$
$$= \frac{4\pi}{\lambda}\left(r_1 - r_2\right)$$

which simplifies to:

$$\phi = \frac{4\pi b}{\lambda} \cdot \cos\left(\theta_0 - \theta\right) \tag{3}$$

in the case of spaceborne systems with $b = |\boldsymbol{b}| << r_1$. (Angles q and q_0 in equation (3) are angles defined in Fig.1). It is evident from (3) that if the phase difference and the baseline parameters (b,$_o$) are known then one can, in principle, obtain the coordinates of P:

$$\begin{cases} x = r \cdot \sin\theta \\ y = h - r \cdot \cos\theta \end{cases} \tag{4.a,b}$$

where

$$\theta = \theta_0 - \cos^{-1}\left(\frac{\phi\,\lambda}{4\pi b}\right). \tag{4c}$$

It should be noted that the phase difference appearing in equation (2) or (3) is the absolute unwrapped phase which cannot be measured directly. In practice, what one does measure is the wrapped phase:

$$\phi_{wrapped} = \phi - 2\pi n \tag{5}$$

where n is sum integer. Here the value of n has to determined independently; a process known as phase unwrapping . It should also be noted the quantities b and $_o$ which characterize the baseline may not be constant for the entire scene.

To generate the interferogram, the two complex images must be first co-registered to within 0.1 pixel accuracy. The (normalized) interferogram is defined as the complex degree of coherence , which for each pair of co-registered complex values s_1 ,s_2, is given by

$$\gamma = \frac{\left\langle s_1 s_2^{*} \right\rangle}{\sqrt{\left\langle s_1 s_1^{*} \right\rangle \cdot \left\langle s_2 s_2^{*} \right\rangle}} \tag{6.a}$$

where the bracket <...> represents an ensemble average.

$$\left\langle s_1 s_2^{*} \right\rangle = \frac{1}{N} \cdot \sum_{k=1}^{N} s_{1,k} \cdot s_{2,k}^{*} \tag{6.b}$$

The phase of is the interferometric phase while its magnitude gives the degree of coherence. To illustrate this, Figs[2] and [3] are the phase and the coherence maps of Singapore generated from a pair of complex images acquired by ERS1/2 satellites.

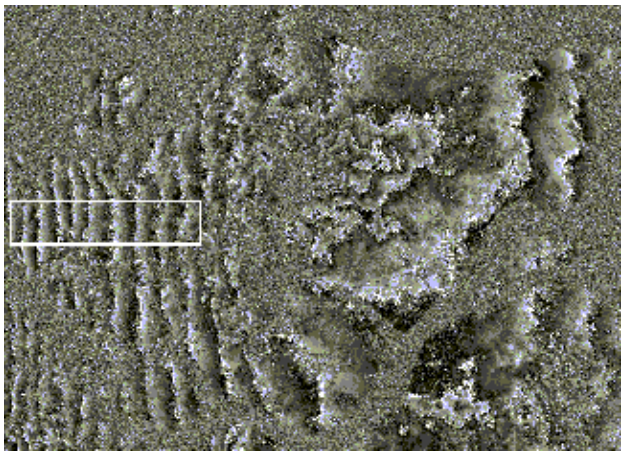

Fig.2: Phase image of Singapore

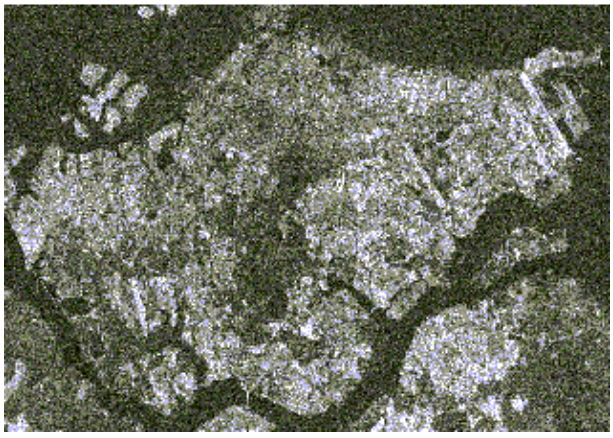

Fig.3: Coherence image of Singapore

3. FOURIER ANALYSIS

In this section we analyse the phase function in the fourier domain. To this end, we begin by considering a flat terrain characterized by the equation

$$r \cdot \cos\theta = h \tag{7}$$

where h represents the height of the satellite. It is advantages to recast eqn (3) in slant range coordinate r since complex images are always acquired in this projection. On substituiting (7) into (3) one obtains

$$\phi(r) = \frac{4\pi b}{\lambda}\left\{\cos\theta_o \frac{h}{r} + \sin\theta_o \frac{\sqrt{r^2 - h^2}}{r}\right\} \tag{8}$$

Here, without loss of generality, we need only to consider values of $_o$ between 0 and . Now the above phase, as mentioned earlier, is the unwrapped phase . It is instructive, at this stage to consider the function

$$\psi(r) = e^{\Psi(r)} \tag{9}$$

which does not distinguish between the wrapped and the unwrapped phases. In other words, one can construct from the measured wrapped phase without losing its validity as being defined for the unwrapped phase. Moreover, its Fourier transform

$$\psi(k) = \int_{r_{min}}^{r_{max}} e^{i(\phi(r) - kr)} dr \tag{10}$$

can also be evaluated analytically using the stationary phase approximation. The limits r_{min} and r_{max} correspond to the range values of the boundary pixels chosen from the interferogram. For instance in the case of the interferogram of Fig.2, if we limit ourselves to a subset defined by the boundary (within the figure), this values correspond to range values of the left-most and the right-most pixels of the rectangle. Before proceeding further, it is instructive to consider the power spectrum of this function for the interferogram of Fig.2.

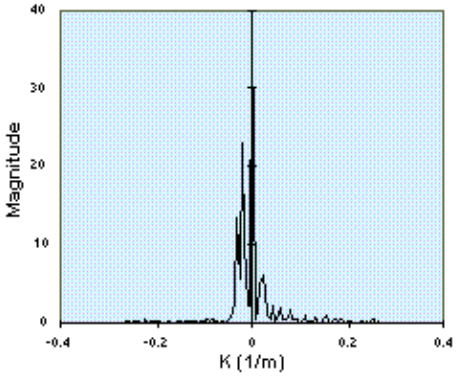

Fig.4 Power spectrum corresponding to (k) evaluated for the phase image of Fig.2.

Here the fourier tansform has been taken for the region enclosed in the rectangle.

Now for the integral (10), with given by (8), the non vanishing contribution comes from values of *k* given by

$$k = \frac{d\phi}{dr} = \frac{4\pi b}{\lambda} \cdot \frac{h}{r^2} \cdot \left\{\sin\theta_o \frac{h}{\sqrt{r^2 - h^2}} - \cos\theta_o\right\} \tag{11}$$

Here it is important to note that the spectrum of (*k*) is bandlimited. This follows from the limits inherent in *r*.

More importantly, the above function displays a monotonic dependence on *r* which is also single-valued. This effectively means that one can expect a spectrum that is characterized by a single band *k* [k_1 , k_2] where k_1 and k_2 are *k* values evaluated at the boundaries of *r*. These features are exemplified by the following simulated results:

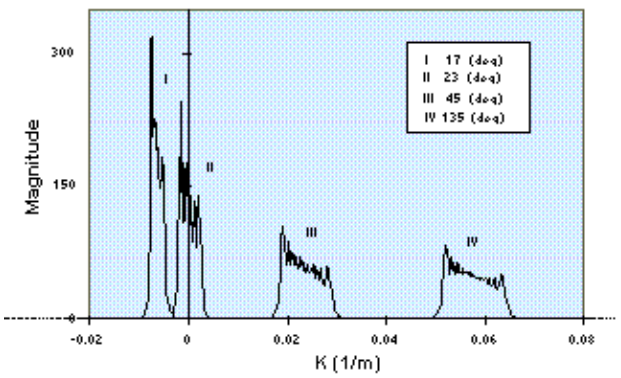

Fig. 5 Power spectrum of (k) obtained for various angles $_o$ with the baseline fixed at 100m.

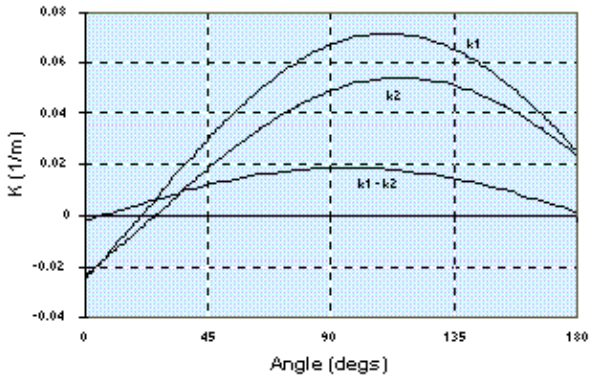

Fig.6: Values of k_1 and k_2 corresponding to k values evaluated at r_{min} and r_{max} respectively, plotted against $_o$.

A closer analysis of k_1 and k_2 further ellucidates the following characteristics:

0 q < q_{min}	q_{min} q q_{max}	q_{max} < q

$k_1 < 0$	$k_1 > 0$	$k_1 > 0$
$k_2 < 0$	$k_2 < 0$	$k_2 > 0$

Here $q_{min} = \cos^{-1}(h/r_{min})$ and $q_{max} = \cos^{-1}(h/r_{max})$.

4. BASELINE DETERMINATION

From measured values of k_1 and k_2 ,the baseline parameters (b,q_0) can be evaluated as follows. By denoting

$$\begin{cases} f(r) = \dfrac{4\pi h}{\lambda r^2} \\ g(r) = \dfrac{h}{\sqrt{r^2 - h^2}} \end{cases} \tag{12.a, b}$$

$$\begin{cases} b_x = b \cdot \sin\theta_0 \\ b_y = b \cdot \cos\theta_0 \end{cases} \tag{13.a, b}$$

in equation (11), one obtains two equations:

$$\begin{pmatrix} f(r_{min}) \cdot g(r_{min}) & f(r_{min}) \\ f(r_{max}) \cdot g(r_{max}) & f(r_{max}) \end{pmatrix} \cdot \begin{pmatrix} b_x \\ b_y \end{pmatrix} = \begin{pmatrix} k_1 \\ k_2 \end{pmatrix} \tag{14}$$

which can be solved for b_x and b_y. The baseline parameters (b, q_0) are then recovered via:

$$b = \sqrt{b_x^2 + b_y^2} \tag{15.a}$$

$$\theta_0 = \tan^{-1}\left(\frac{b_x}{b_y}\right) \tag{15.b}$$

The analysis so far is valid only for a terrain which is flat. In most realistic situations, however this is often not the case. In the following we generalize the equations above, so that its applicability can be extended to a terrain which is not flat.

To the end, we begin by replacing (8) by:

$$\phi(k) = \frac{4\pi b}{\lambda} \cdot \left\{ \cos\theta_0 \frac{h - y(x)}{\sqrt{x^2 + (h - y(x))^2}} + \sin\theta_0 \frac{x}{\sqrt{x^2 + (h - y(x))^2}} \right\} \tag{16}$$

where y a function of x, is assumed to be known. In the present case, it is convenient to recast the integral (10) back to the ground range coordinates:

$$\begin{aligned} \Psi(k) &= \int_{r_{min}}^{r_{max}} e^{i(\phi(r) - kr)} dr \\ &= \int_{x_{min}}^{x_{max}} e^{i\left[\phi(x) - k\sqrt{x^2 + (h-y)^2}\right]} \cdot \left|\frac{dr}{dx}\right| \cdot dx \end{aligned} \tag{17}$$

where x_{min} and x_{max} are related to r_{min} and r_{max} respectively through the equation $r = \sqrt{x^2 + (h-y)^2}$.

Here, if the Jacobian does not vary rapidly within the limits of the integration, one can apply the method of stationary phase to evaluate the spectral function. Indeed by setting:

$$\frac{d}{dx}\left[\phi(x) - k\sqrt{x^2 + (h-y)^2}\right] = 0 \tag{18}$$

one obtains:

$$k = \frac{\dfrac{d\phi}{dx} \cdot \sqrt{x^2 + (h-y)^2}}{x - (h-y)\dfrac{dy}{dx}} \tag{19}$$

which can be further reduced to:

$$k = \frac{4\pi b}{\lambda}\left\{\frac{(h-y)\sin\theta_0 - x\cdot\cos\theta_0}{x^2+(h-y)^2}\right\}\cdot\left\{\frac{h-y+x\cdot\frac{dy}{dx}}{x-(h-y)\cdot\frac{dy}{dx}}\right\} \quad (20)$$

Again, this equation is to be taken within the limits of *x* imposed in (17). It is interesting to note that when *y*=0 the above equation reduces to (11). Now, for the present case, the above function, depending on y, may not be monotonic or even single valued for the specified range of *x* values.

If this happens to be the case, equation (20) can be used in determining a subset over which these conditions are satisfied.

These boundary values can then be fed into (20) to yield the corresponding k values. The two equation thus generated can be solved to yield *b* and q_0 as in the flat case.

Figs.7 and 8 illustrate the power spectrum of two different terrain types.

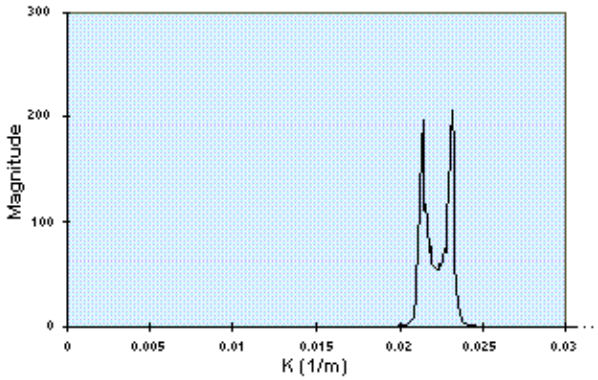

Fig. 7: Power spectrum corresponding to a terrain modelled by y = c.exp[-(x-m)/2s^2], with c=500, m=334012, s=137471, x_{max}=374425.44, x_{min}=293599.20, b=100, q_0=90.

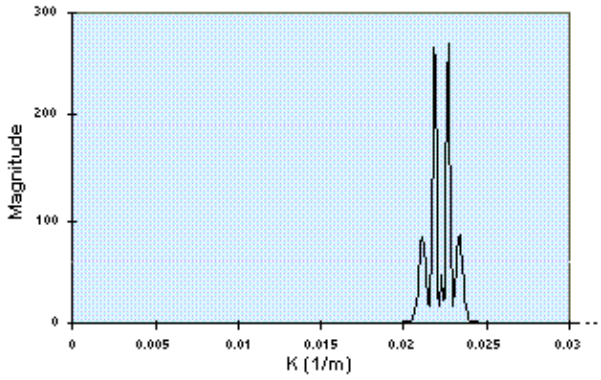

Fig. 8: Power spectrum corresponding to a terrain modelled by y = c.(1-cos[6.p.(x-x_{min}) / (x_{max}-x_{min})]), with c=100, x_{max}=374425.44, x_{min}=293599.20, b=100, q_0=90.

To summarize briefly, we have shown how the baseline can be determined from an interferogram. Traditionally, the baseline parameters usually serve as inputs in DEM generation. Here, we do the converse. In other word, from knowledge on the ground terrain, we show that the baseline (both the normal and perpendicular components) can be obtained from a detailed analysis of the interferometric fringes. This is particulary useful in differential interferometric work where the DEM is assumed known, and an accurate value of the baseline is required.

REFERENCES

[1] L.C. Graham, "Synthetic interferometer